

# Highly heterogeneous Precambrian basement under the central Deccan Traps, India: Direct evidence from xenoliths in dykes

Ranjini Ray<sup>a</sup>, Anil D. Shukla<sup>b</sup>, Hetu C. Sheth<sup>a,\*</sup>, Jyotiranjana S. Ray<sup>b</sup>, Raymond A. Duraiswami<sup>c</sup>,  
Loyc Vanderkluisen<sup>d</sup>, Chandramohan S. Rautela<sup>b</sup>, Jyotirmoy Mallik<sup>a</sup>

<sup>a</sup> Department of Earth Sciences, Indian Institute of Technology (IIT) Bombay, Powai, Mumbai 400 076, India

<sup>b</sup> Planetary and Geosciences Division, Physical Research Laboratory (PRL), Navrangpura, Ahmedabad 380 009, India

<sup>c</sup> Department of Geology, University of Pune, Ganesh Khind, Pune 411 007, India

<sup>d</sup> Department of Geology and Geophysics, School of Ocean and Earth Science and Technology (SOEST), University of Hawaii, Honolulu, USA

Received 30 May 2007; received in revised form 14 October 2007; accepted 17 October 2007

Available online 17 November 2007

## Abstract

Crustal or mantle xenoliths are not common in evolved, tholeiitic flood basalts that cover huge areas of the Precambrian shields. Yet, the occasional occurrences provide the most direct and unequivocal evidence on basement composition. Few xenolith occurrences are known from the Deccan Traps, India, and inferences about the Deccan basement have necessarily depended on geophysical studies and geochemistry of Deccan lavas and intrusions. Here, we report two basalt dykes (Rajmane and Talwade dykes) from the central Deccan Traps that are extremely rich in crustal xenoliths of great lithological variety (gneisses, quartzites, granite mylonite, felsic granulite, carbonate rock, tuff). Because the dykes are parallel and only 4 km apart, and only a few kilometres long, the xenoliths provide clear evidence for high small-scale lithological heterogeneity and strong tectonic deformation in the Precambrian Indian crust beneath. Measured  $^{87}\text{Sr}/^{86}\text{Sr}$  ratios in the xenoliths range from 0.70935 (carbonate) to 0.78479 (granite mylonite). The Rajmane dyke sampled away from any of the xenoliths shows a present-day  $^{87}\text{Sr}/^{86}\text{Sr}$  ratio of 0.70465 and initial (at 66 Ma) ratio of 0.70445. The dyke is subalkalic and fairly evolved (Mg No. = 44.1) and broadly similar in its Sr-isotopic and elemental composition to some of the lavas of the Mahabaleshwar Formation. The xenoliths are comparable lithologically and geochemically to basement rocks from the Archaean Dharwar craton forming much of southern India. As several lines of evidence suggest, the Dharwar craton may extend at least 350–400 km north under the Deccan lava cover. This is significant for Precambrian crustal evolution of India besides continental reconstructions.

© 2007 International Association for Gondwana Research. Published by Elsevier B.V. All rights reserved.

**Keywords:** Continental crust; Precambrian; Xenolith; Deccan; India

## 1. Introduction

The Precambrian Indian shield is one of the oldest in the world. At least six Archaean to early Proterozoic cratonic nuclei, and several fold belts, are recognized in India, and several major rift zones traverse peninsular India along Precambrian structural trends (Fig. 1; Radhakrishna and Naqvi, 1986; Naqvi and Rogers, 1987; Bhaskar Rao et al., 1992; Mahadevan, 1994; Rogers and Santosh, 2004; Sheth and Pande, 2004; Santosh et al., 2005; Manikyamba and Khanna, 2007). The Deccan flood basalts, ~66 m.y. in age (e.g., Pande, 2002) cover and effect-

ively hide the basement rocks over a huge area (500,000 km<sup>2</sup>) of western and central India. They are best exposed in the Western Ghats region (Fig. 1), where a stratigraphic thickness of ~3,000 m has been divided into various formations and sub-groups (Table 1; Subbarao and Hooper, 1988 and references therein).

Whereas xenoliths in lavas and intrusions provide direct evidence on basement composition (e.g., Rudnick, 1992; Rudnick and Fountain, 1995), very few occurrences of mantle or crustal xenoliths are known in the Deccan Traps, because the basalt lava pile is largely made up of fairly evolved tholeiites that may be products of significant crystal fractionation in magma chambers (cf. Farahat et al., 2007). Our knowledge of the basement of the huge province is therefore necessarily indirect and inferential,

\* Corresponding author. Tel.: +91 22 25767264; fax: +91 22 25767253.

E-mail address: [hesheth@iitb.ac.in](mailto:hesheth@iitb.ac.in) (H.C. Sheth).

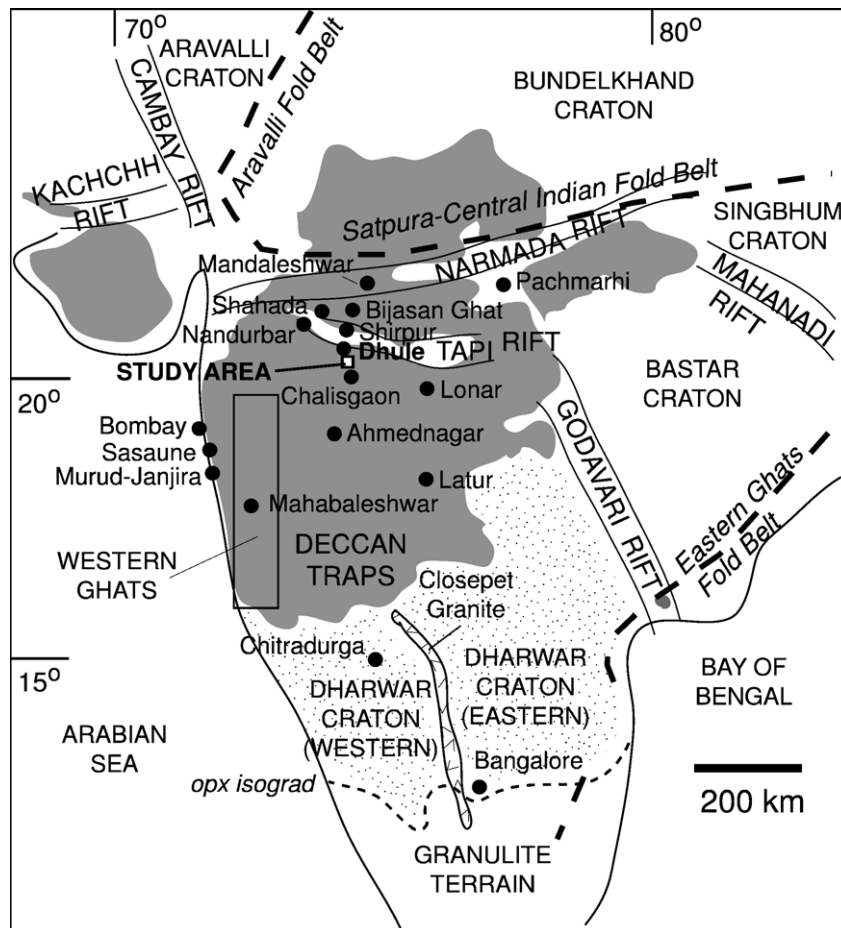


Fig. 1. Schematic map of India showing the outcrop of the Deccan Traps (shaded), the Precambrian cratonic nuclei and fold belts (mostly Proterozoic, heavy dashed lines), as well as the Proterozoic and Phanerozoic rift zones. Localities mentioned in the text are also shown. Based on Radhakrishna and Naqvi (1986), Naqvi and Rogers (1987), and Senthil Kumar et al. (2007).

and derives from geophysical studies (e.g., Rao and Reddy, 2002; Rai and Thiagarajan, 2007) as well as the geochemistry of the Deccan lavas and dykes themselves. For example, lavas of the Bushe Formation with high initial  $^{87}\text{Sr}/^{86}\text{Sr}$  ratios are inferred to have been contaminated by ancient, Rb-rich, granitic

upper crust, whereas the low- $^{206}\text{Pb}/^{204}\text{Pb}$  Mahabaleshwar Formation lavas have been considered possibly contaminated by U-poor, lower crustal granulites (e.g., Mahoney et al., 1982; Mahoney, 1988; Peng et al., 1994). Here we report direct, significant evidence on basement composition available from highly varied crustal xenoliths in two basaltic dykes in the central Deccan Traps.

Table 1  
Stratigraphy and initial Sr isotopic values (at 66 Ma) for the Deccan flood basalts, Western Ghats

| Group         | Sub-group | Formation                | $^{87}\text{Sr}/^{86}\text{Sr}_{(66 \text{ Ma})}$ |
|---------------|-----------|--------------------------|---|
|               | Wai       | Desur* (~100 m)          | 0.7072–0.7080                                     |
|               |           | Panhala (>175 m)         | 0.7046–0.7055                                     |
|               |           | Mahabaleshwar (280 m)    | 0.7040–0.7055                                     |
|               |           | Ambenali (500 m)         | 0.7038–0.7044                                     |
|               |           | Poladpur (375 m)         | 0.7053–0.7110                                     |
| Deccan Basalt | Lonavala  | Bushe (325 m)            | 0.7078–0.7200                                     |
|               |           | Khandala (140 m)         | 0.7071–0.7124                                     |
|               | Kalsubai  | Bhimashankar (140 m)     | 0.7067–0.7076                                     |
|               |           | Thakurvadi (650 m)       | 0.7067–0.7112                                     |
|               |           | Neral (100 m)            | 0.7062–0.7104                                     |
|               |           | Jawhar–Igatpuri (>700 m) | 0.7085–0.7128                                     |

\*The Desur is considered by many as a “Unit” of the Panhala Formation itself. Table based on Subbarao and Hooper (1988) and references therein, and Peng et al. (1994).

## 2. Field geology

Many large dykes in the Deccan Traps trend ENE–WSW, the strike of the Satpura–Central Indian Tectonic Zone, and define a particularly fine and dense dyke swarm in the Nandurbar–Dhule region in the central Deccan (Fig. 1; Ray et al., 2007). Whereas none of these dykes contain any obvious xenoliths, we have found two ~E–W basalt dykes that outcrop a little to the south of the Nandurbar–Dhule swarm, and contain profuse xenoliths. These dykes outcrop some 30 km south of Dhule city and can be easily approached by the National Highway 211 connecting Dhule to Chalisgaon (Fig. 2). The dykes, spaced 4 km apart, form linear ridges over a largely flat lava landscape due to their greater resistance to erosion. These host lavas apparently belong to the Khandala Formation of the Western

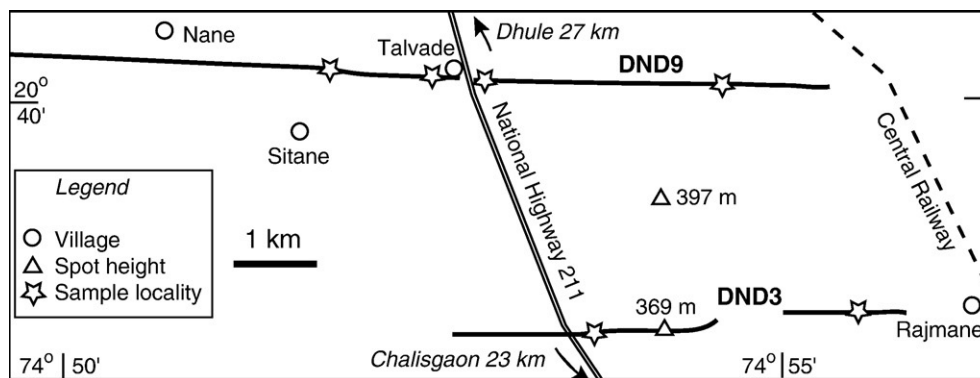


Fig. 2. Location map of the Rajmane and Talwade dykes. The terrain is quite flat.

Ghats stratigraphy (see Fig. 6 of Subbarao et al., 1994; Melluso et al., 2004).

The thicker of the two dykes (named here the Rajmane dyke, DND3) is segmented, with a total length of 5.5 km and a N85° trend. It is 6.5 m wide, vertical, and forms a large ridge across the N. H. 211 rising ~15 m above ground level (Fig. 3A, B). The xenoliths in the dyke form large boulders, conspicuous even from 2 km away, curiously concentrated in the upper part of the dyke along the ridge crest. The roadcut clearly shows that they are absent in the lower exposed part of the dyke (Fig. 3B). Apparently the xenoliths have floated upwards in the dyke magma due to their low densities, consistent with the observed rock types. The xenoliths comprise granite mylonite (Fig. 3C, appearing granitic in outcrop), banded gneiss, sometimes permeated by the dyke magma (Fig. 3D), as well as augen gneiss (Fig. 3E) containing alkali feldspar porphyroblasts up to 3 cm in size. Vein quartz fragments and very fine-grained quartzites also occur in abundance, many forming long ribbons or prisms with sharp boundaries (Fig. 3F), or more equidimensional masses with quenched melt around them (Fig. 3G,H). Rudnick and Fountain (1995) observe that felsic xenoliths from the lower crust will survive transport by basaltic melts if they are below their solidi at the time of xenolith entrainment, and if the melt ascent rates are rapid. Some of the fine-grained quartzite xenoliths clearly show the ingress of melt along fractures in them (Fig. 3H). The whole Rajmane dyke, and some of the larger xenoliths therein, have been intruded by many small basaltic dykelets. Fig. 3I shows a laterally terminating mafic dykelet in a single augen gneiss block >3 m in size that outcrops on the dyke ridge only ~50 m from the highway. Very similar outcrops of many small basic dykelets intruding granitic and quartz-rich rafts and their host dyke have been described by Duraiswami and Karmalkar (1996) from Mandaleshwar (Fig. 1), on the Narmada River.

The second dyke, the Talwade dyke (DND9), outcrops 4 km north of the Rajmane dyke, and runs almost E–W right through the village Talwade (Fig. 2). This dyke is 18 km long and is only 3 m wide, and exposes only about 2 m of its vertical dimension (Fig. 3J, K). The xenoliths in the Talwade dyke show greater lithological variety. Large quartzite xenoliths similar to those in the Rajmane dyke, including some showing folds, are seen in the Talwade dyke. Granite gneiss is the most dominant rock,

constituting ~50% of the xenoliths, and generally forming small angular xenoliths showing distinct foliation. However, it also occurs as larger blocks (~170 × 67 cm) and slender tabular rafts (~106 × 35 cm). Some of the large gneissic xenoliths are intruded by ~1-cm-thick mafic veins across the foliation. A few gneissic xenoliths preserve foliation patterns that resemble pygmatic folding. The non-foliated or feebly foliated xenoliths were called granitic in the field. A large (~353 × 229 cm) granitic (non-foliated) xenolith shows bands of fine-grained mylonite. The Talwade dyke is also strewn with fragments of vein quartz, which occur as angular and elongated pieces. Though fractured, they stand out boldly in outcrop as they are resistant to weathering. The xenolith density is often so high in the Talwade dyke that the dyke is transformed into a hybrid rock (Fig. 3L). Besides the above, three very different rock types were also found in the Talwade dyke: one sample of a feldspathic (granulite?) xenolith (~25 × 12 cm), one calcareous rock (~21 × 14 cm) and a fine-grained tuff (~16 × 1 cm).

Fig. 4 shows the frequency distribution of the different lithological types represented in the Talwade and Rajmane xenoliths.

### 3. Petrography

Petrographic studies reveal that the variety of rock types represented by the xenoliths is much greater than apparent in the field, though all rock types do not occur in equal abundance, varieties of gneiss and quartzite being the most abundant. The dykes themselves are dark, fine-grained and relatively fresh basalts, mostly aphyric. Dyke DND3 (Fig. 5A) shows a few multiply twinned plagioclase feldspar phenocrysts in a groundmass made up of laths of plagioclase partially enclosed by clinopyroxene crystals, forming sub-ophitic texture.

Fig. 5B shows a small fragment of the quartzite surrounded by the basalt melt (sample 3X1). Sample 3X2 (Fig. 5C) is augen gneiss. Sample 3X3 (Fig. 5D) is a granite mylonite with a typical porphyroclastic texture, in which the quartz grains have been considerably deformed and show undulose extinction, and alkali feldspars are highly altered. Samples 3X4, the banded gneiss, does not show a foliation on the scale of the thin section (Fig. 5E), but a distinct layering in outcrop. 3X5 is fine-grained quartzite (Fig. 5F). Sample 78 (Fig. 5G–H) is a very interesting



Fig. 3. The Rajmane and Talwade dykes and their xenoliths in outcrop. Photos 3A to 3I show the Rajmane dyke; 3J to 3L the Talwade dyke. See text for details.

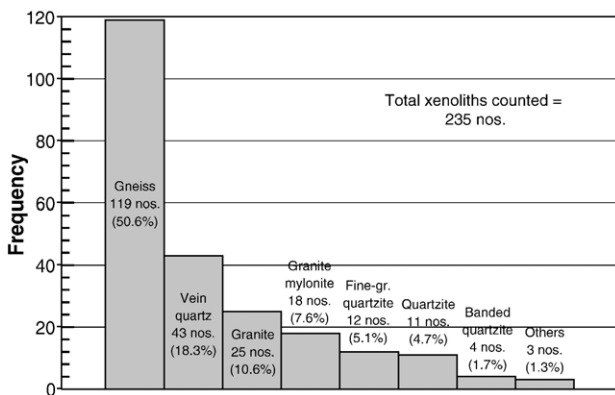


Fig. 4. Overall xenolith frequency distribution in the Talwade and Rajmane dykes for a total of 235 xenoliths counted. Note that the rock names are purely field terms.

quartzite in which the individual quartz grains show fine, needle-like overgrowths. The needles show the same optical orientations as the grains from which they project. The matrix of the rock is made up of the dyke basalt which is full of such needles. There are some feldspar grains as well. We believe that the needles are probably paramorphs after tridymite—at depth there may have been a quartz–tridymite inversion due to the magmatic heat, and the tridymites nucleated on quartz grains and grew into the basalt melt. A very similar phenomenon has been described and illustrated by Barker (2000) for xenoliths in a basic sill from Lajitas, Texas (compare his Fig. 7). Sample 26 (Fig. 5I) is a schistose quartzite. The feldspathic rock sample X8 (Fig. 5J) is almost completely made up of plagioclase. The plagioclase grains are interlocking and completely anhedral. This is granoblastic texture, indicating metamorphic recrystallization (Best, 2003), and the name felsic or feldspathic granulite seems appropriate for the rock. The carbonate rock X79 (Fig. 5K), probably a recrystallized limestone, gives a clear

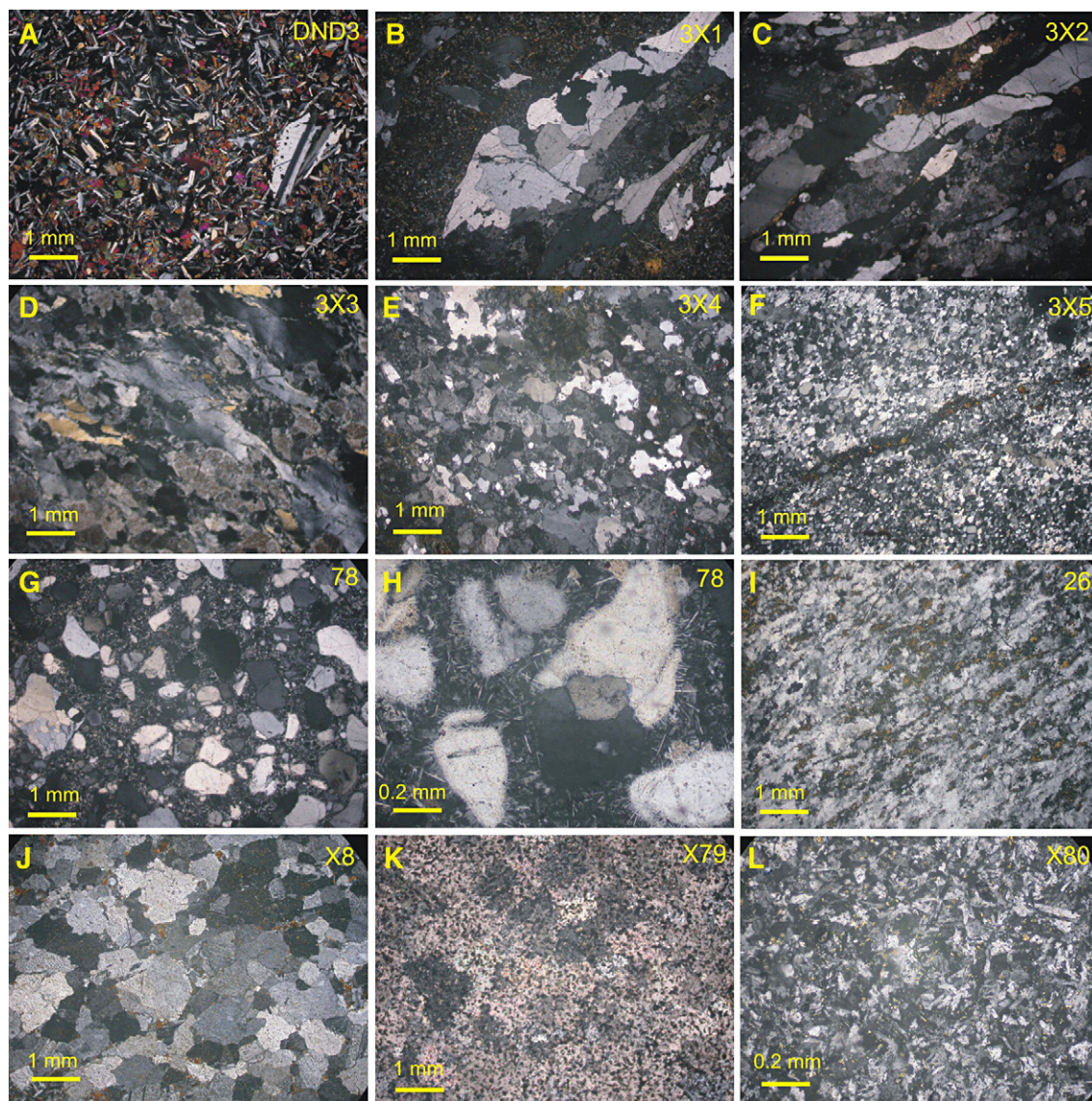


Fig. 5. Photomicrographs, all taken between crossed nicols. The xenoliths in 5B through 5F come from the Rajmane dyke DND3. The rest come from the Talwade dyke DND9.

effervescence on reaction with dilute hydrochloric acid. Finally, sample X80 (Fig. 5L) is evidently a plagioclase–pyroxene tuff from its appearance in hand sample and in thin section. Additionally, there are a few quite small xenoliths with a very confusing aspect and containing quartz, feldspar, amphibole needles, highly altered olivines, and Fe-oxides. They appear to be intimate physical mixtures of the basalt magma and fragmented xenoliths or xenocrysts.

#### 4. Geochemistry

The Rajmane dyke (sample DND3) and some of the xenoliths were analyzed for major and trace element compositions at the National Facility for Planetary Science and Exploration Programme of the Indian Space Research Organization (ISRO), located at the Physical Research Laboratory. The major and trace elements were analyzed by powder-pressed X-ray fluorescence (XRF) spectrometry (Axios, from Panalytical

Limited) and inductively coupled plasma mass spectrometry (ICPMS, Thermoelectron X-Series II). For calibrating for major oxides on XRF we used AGV-1, BCR-2, BHVO-2, BIR-1, G-2, GSP-1, STM-1 and W-2 international rock standards, whereas BHVO-2 and W-2 were used as calibration standards for trace element concentrations on ICPMS. Sr isotopic ratios were measured using an ISOPROBE-T thermal ionization mass spectrometer and tantalum filaments at the Physical Research Laboratory. Table 2 presents these data along with data on analytical accuracy and precision.

The Rajmane dyke was sampled in the highway roadcut several metres below the bouldery xenoliths at the top, hoping that the composition would be as pristine (free from xenolith influence) as possible. As expected, this sample is not SiO<sub>2</sub>-rich. Recalculated (LOI-free) SiO<sub>2</sub> and alkali contents indicate that the dyke is subalkalic (like the overwhelming majority of Western Ghats Deccan lavas, Sheth, 2005) on the total alkali–silica diagram (Le Bas et al., 1986) (not shown). Assuming 85%

Table 2  
Major and trace element and  $^{87}\text{Sr}/^{86}\text{Sr}$  data for the Rajmane dyke, xenoliths, and standards

| Sample                           | DND-3<br>Rajmane dyke | 3X2<br>Augen gneiss | 3X3<br>Granite mylonite | 3X4<br>Banded gneiss | 3X5<br>Fine-gr. quartzite | X79<br>Carbon. | Std.      |               | Std.     |               |
|----------------------------------|-----------------------|---------------------|-------------------------|----------------------|---------------------------|----------------|-----------|---------------|----------|---------------|
|                                  |                       |                     |                         |                      |                           |                | G-2 Meas. | $\pm 2\sigma$ | G-2 Ref. | $\pm 2\sigma$ |
| <i>wt. %</i>                     |                       |                     |                         |                      |                           |                |           |               |          |               |
| SiO <sub>2</sub>                 | 48.27                 | 63.24               | 69.91                   | 70.22                | 87.11                     | 15.97          | 68.99     | 0.17          | 69.14    | 0.30          |
| TiO <sub>2</sub>                 | 3.38                  | 0.57                | 0.03                    | 0.15                 | 0.07                      | 0.33           | 0.47      | 0.01          | 0.48     | 0.03          |
| Al <sub>2</sub> O <sub>3</sub>   | 12.73                 | 13.51               | 13.49                   | 13.49                | 6.64                      | 3.56           | 15.47     | 0.01          | 15.39    | 0.30          |
| Fe <sub>2</sub> O <sub>3</sub> T | 15.14                 | 3.98                | bdl                     | 1.22                 | 0.40                      | 3.76           | 2.68      | 0.01          | 2.66     | 0.14          |
| MnO                              | 0.19                  | 0.05                | 0.01                    | 0.01                 | 0.01                      | 0.04           | 0.03      | 0.01          | 0.03     | 0.01          |
| MgO                              | 5.10                  | 0.67                | bdl                     | bdl                  | bdl                       | 5.10           | 0.83      | 0.02          | 0.75     | 0.03          |
| CaO                              | 9.65                  | 2.68                | 0.38                    | 1.21                 | 0.93                      | 39.21          | 1.96      | 0.01          | 1.96     | 0.08          |
| Na <sub>2</sub> O                | 1.97                  | 2.98                | 1.59                    | 2.93                 | 0.17                      | 0.01           | 4.24      | 0.01          | 4.08     | 0.13          |
| K <sub>2</sub> O                 | 0.61                  | 3.75                | 7.93                    | 4.62                 | 0.04                      | 0.23           | 4.49      | 0.01          | 4.48     | 0.13          |
| P <sub>2</sub> O <sub>5</sub>    | 0.39                  | 0.16                | bdl                     | 0.01                 | 0.09                      | 0.11           | 0.12      | 0.01          | 0.14     | 0.01          |
| Total                            | 97.43                 | 91.58               | 93.33                   | 93.87                | 95.47                     | 68.32          | 99.30     |               | 99.11    |               |
|                                  |                       |                     |                         |                      |                           |                | BHVO-2    |               | BHVO-2   |               |
|                                  |                       |                     |                         |                      |                           |                | Meas.     | $\pm 2\sigma$ | Ref.     | $\pm 2\sigma$ |
| <i>ppm</i>                       |                       |                     |                         |                      |                           |                |           |               |          |               |
| Rb                               | 15.7                  | 90.2                | 267                     | 95.2                 | 3.22                      | 14.2           | 11.7      | 0.2           | 10.1     | 1.20          |
| Ba                               | 135                   | 1298                | 1967                    | 1011                 | 54.2                      | 237            | 119       | 1.2           | 128      | 8.00          |
| Th                               | 2.13                  | 1.39                | 0.43                    | 0.21                 | 0.20                      | 5.21           | 1.20      | 0.02          | 1.18     | 0.18          |
| Nb                               | 16.0                  | 10.2                | 0.24                    | 1.25                 | 0.33                      | 6.15           | 16.0      | 0.26          | 16.4     | 1.40          |
| Ta                               | 0.92                  | 0.46                | 0.02                    | 0.04                 | 0.01                      | 0.37           | 0.89      | 0.01          | 0.94     | 0.14          |
| La                               | 17.2                  | 41.0                | 6.67                    | 17.9                 | 0.96                      | 18.6           | 14.1      | 0.18          | 15.6     | 1.20          |
| Ce                               | 42.1                  | 77.0                | 5.86                    | 20.7                 | 1.17                      | 36.0           | 37.6      | 0.40          | 37.0     | 2.00          |
| Pr                               | 6.48                  | 9.57                | 0.33                    | 1.86                 | 0.04                      | 4.34           | 5.40      | 0.06          | 5.00     | 0.60          |
| Sr                               | 219                   | 284                 | 170                     | 179                  | 77.7                      | 1025           | 386       | 4.8           | 382      | 20            |
| Nd                               | 28.9                  | 35.0                | 0.89                    | 5.64                 | 0.58                      | 15.4           | 23.8      | 0.20          | 24.0     | 2.00          |
| Zr                               | 205                   | 122                 | 1.77                    | 4.27                 | 4.04                      | 62.0           | 151       | 1.40          | 160      | 16.0          |
| Hf                               | 5.13                  | 2.86                | 0.04                    | 0.13                 | 0.10                      | 1.53           | 3.99      | 0.06          | 4.10     | 0.80          |
| Sm                               | 7.39                  | 6.21                | 0.10                    | 0.70                 | 0.14                      | 2.88           | 5.70      | 0.08          | 5.80     | 1.00          |
| Eu                               | 2.19                  | 2.22                | 1.32                    | 1.04                 | 0.05                      | 0.63           | 1.99      | 0.02          | 2.00     | 0.20          |
| Gd                               | 7.80                  | 5.68                | 0.14                    | 0.71                 | 0.17                      | 2.72           | 6.20      | 0.06          | 5.90     | 0.80          |
| Tb                               | 1.23                  | 0.71                | 0.01                    | 0.07                 | 0.02                      | 0.37           | 0.82      | 0.02          | 0.86     | 0.12          |
| Dy                               | 7.67                  | 3.98                | 0.09                    | 0.37                 | 0.18                      | 2.23           | 4.80      | 0.06          | 4.90     | 0.80          |
| Ho                               | 1.51                  | 0.76                | 0.02                    | 0.07                 | 0.04                      | 0.44           | 0.89      | 0.02          | 0.91     | 0.12          |
| Er                               | 3.97                  | 1.96                | 0.04                    | 0.19                 | 0.09                      | 1.19           | 2.22      | 0.02          | 2.30     | 0.40          |
| Tm                               | 0.54                  | 0.25                | 0.01                    | 0.02                 | 0.01                      | 0.17           | 0.29      | 0.02          | 0.30     | 0.10          |
| Yb                               | 3.72                  | 1.68                | 0.02                    | 0.17                 | 0.07                      | 1.18           | 1.91      | 0.04          | 2.00     | 0.40          |
| Lu                               | 0.51                  | 0.22                | 0.003                   | 0.03                 | 0.01                      | 0.16           | 0.25      | 0.01          | 0.26     | 0.08          |
| Sc                               | 36.8                  | 7.16                | 0.19                    | 1.05                 | 0.63                      | 11.4           | 29.4      | 0.44          | 31.0     | 2.00          |
| V                                | 434                   | 51.4                | 1.88                    | 13.1                 | 6.73                      | 104            | 318       | 6.0           | 329      | 18            |
| Cr                               | 93                    | 9.8                 | bdl                     | 1.4                  | 1.6                       | 64             | 275       | 4.0           | 285      | 28            |
| Co                               | 53                    | 8.6                 | 0.14                    | 1.8                  | 2.0                       | 13             | 44        | 0.76          | 47       | 4.0           |
| Ni                               | 131                   | 7.8                 | bdl                     | 0.85                 | 1.9                       | 22             | 105       | 2.2           | 112      | 18            |
| Zn                               | 225                   | 49                  | bdl                     | 14                   | 8.6                       | 37             | 101       | 1.6           | 107      | 52            |
|                                  |                       |                     |                         |                      |                           |                | BHVO-2    |               | BHVO-2   |               |
| $^{87}\text{Sr}/^{86}\text{Sr}$  | 0.70465               | 0.72801             | 0.78479                 | 0.73324              | 0.71426                   | 0.70935        | 0.70347   |               | 0.70348  |               |
| meas.                            |                       |                     |                         |                      |                           |                |           |               |          |               |
| $^{87}\text{Rb}/^{86}\text{Sr}$  |                       |                     |                         |                      |                           |                |           |               |          |               |
| calc.                            | 0.2075                | 0.9212              | 4.581                   | 1.543                | 0.1200                    | 0.0401         |           |               |          |               |
| $^{87}\text{Sr}/^{86}\text{Sr}$  |                       |                     |                         |                      |                           |                |           |               |          |               |
| 66 Ma                            | 0.70445               | 0.72715             | 0.78050                 | 0.73179              | 0.71415                   | 0.70931        |           |               |          |               |

Notes: Analyses performed at the Physical Research Laboratory, Ahmedabad. G-2 meas. is average of three measurements. Value of  $^{87}\text{Sr}/^{86}\text{Sr}$  for standard NBS987 over a 2-year period ( $n=72$ ) is  $0.710230 \pm 0.000003$  ( $2\sigma_{\text{SE}}$ ). bdl, below detection limit. Reference values for G-2: U. S. Geological Survey, BHVO-2: Gao et al. (2002) and Weis et al. (2005).

of the total Fe to be in the FeO form, and using LOI-free values, the FeO value (after due Fe<sub>2</sub>O<sub>3</sub>–FeO conversion) is 11.88. This gives a Mg Number (the molar ratio of MgO to MgO+FeO) of 44.1, indicating a considerably evolved magma. If the parental melt of this magma were picritic, significant olivine ( $\pm$ clinopyroxene) fractionation occurred, necessarily prior to the entrain-

ment of the profuse middle/lower crustal xenoliths. The major oxide totals for the xenoliths are somewhat below 100% (much below 100% for X79, the carbonate xenolith), and volatiles would easily account for the difference. The augen gneiss (3X2), granite mylonite (3X3) and banded gneiss (3X4) are very similar in composition, and have Al<sub>2</sub>O<sub>3</sub> contents  $\sim 13.5\%$ .

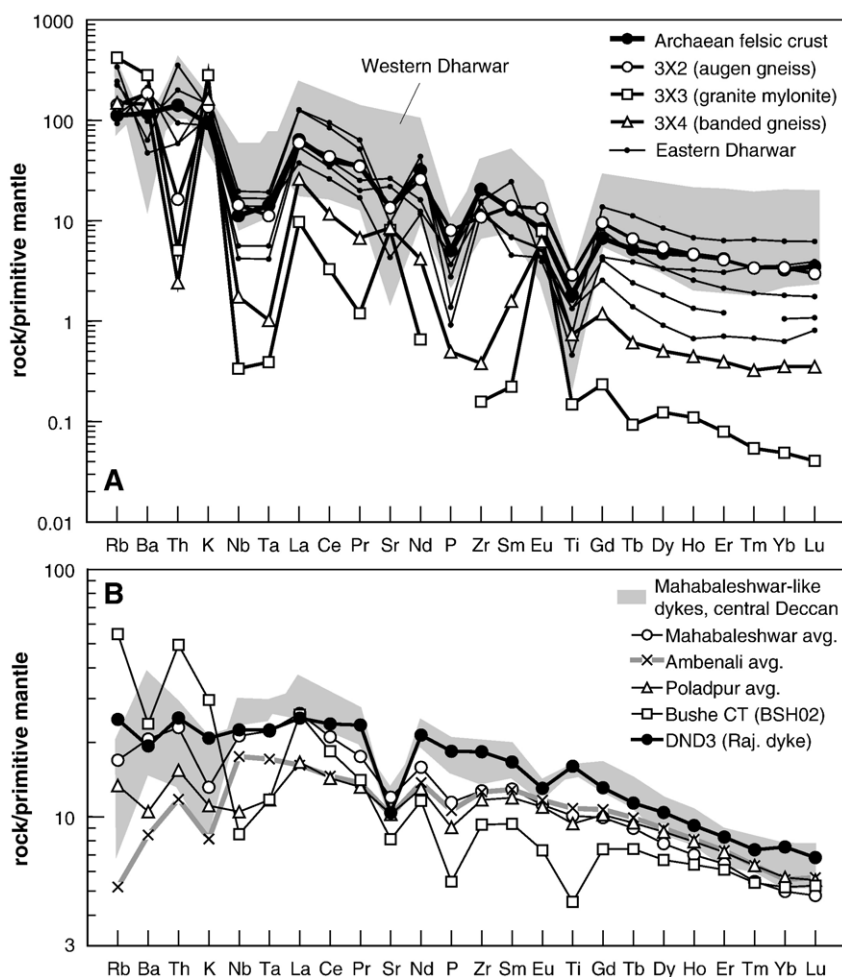


Fig. 6. (A) Primitive mantle normalized multi-element patterns for the xenoliths, average Archaean felsic crust (Rudnick and Fountain, 1995), and late Archaean granitoids from the Western and Eastern Dharwar cratons (Jayananda et al., 2000, 2006). (B) Patterns for the Rajmane dyke DND3 and various Deccan formation averages (e.g., Sheth et al., 2004). CT, Chemical Type. The normalizing values are from Sun and McDonough (1989). Shaded field covers dykes in the Shirpur–Bijasan Ghat area (samples SH41, SH51, SH25) that are broadly Mahabaleshwar-like (geochemically and isotopically); data sources are Chandrasekharam et al. (1999, 2000) and Sheth et al. (2004).

Fig. 6 shows the primitive mantle normalized multi-element patterns for the xenoliths and dyke DND3. The augen gneiss (Fig. 6a) has a pattern closely similar to the average Archaean felsic crust (Rudnick and Fountain, 1995). The negative Nb–Ta, Sr, P and Ti anomalies in these patterns correspond well. The Archaean Dharwar craton is exposed to the south of the Deccan lavas and extends an unknown distance under them (Fig. 1). Late Archaean granitoids from the Western and Eastern Dharwar craton (Jayananda et al., 2000, 2006) show quite similar patterns to the augen gneiss 3X2. The granite mylonite and the banded gneiss, however, have patterns strikingly different from that of average Archaean felsic crust, and these patterns are very highly fractionated ( $Rb_N/Lu_N$  equals 10,500 in the granite mylonite). The mylonite shows strong spikes at both Sr and Eu, and the banded gneiss smaller ones. All three xenoliths are similar, however, in the pronounced troughs they show in their multi-element patterns at Th, Nb and Ta.

The multi-element pattern for dyke DND3 is somewhat close to the patterns of the Mahabaleshwar and Ambenali formations of the Deccan Traps (Fig. 6B), though the similarity is only in a few elements. The fit of the DND3 pattern to the Ambenali

pattern would improve (but not sufficiently) if both were compared at the same  $Lu_N$  value; in the absence of Pb concentration data for DND3 it is not easy to say whether it has a greater affinity to the Ambenali or Mahabaleshwar (cf. Mahoney et al., 2000; Sheth et al., 2004; Bondre et al., 2006). However, Mahabaleshwar-type dykes (in elemental and Nd–Sr–Pb isotopic composition) have been known from the Shahada–Shirpur–Bijasan Ghat region N–NE of Dhule (Fig. 1; Chandrasekharam et al., 1999; Sheth et al., 2004; Vanderkluyesen et al., 2006), far north of the exposures of the Mahabaleshwar Formation, and the dyke DND3 is comparable in many elements to them (Fig. 6). The DND3 pattern shows significant negative anomalies at both Sr and Eu, explained by plagioclase fractionation, such fractionation consistent with the actual presence of plagioclase phenocrysts (Fig. 5A).

The DND3 pattern is considerably different from the patterns for the crustally contaminated magma types in the Deccan, such as the Poladpur and Bushe Formation lavas (Fig. 6B). These crustally contaminated lavas define elongated fields—mixing arrays—between the Ambenali magma type and lithospheric materials on binary plots involving several elements, element

ratios, or isotopic ratios (e.g., Lightfoot et al., 1990; Peng et al., 1994). Fig. 7 shows such a plot of Th/Yb vs. Ta/Yb showing the data for the sample DND3 and several Western Ghats formations, as well as the xenoliths analyzed in the present study, mafic granulite xenoliths from Murud–Janjira (Fig. 1), late Archaean granitoids from the Western Dharwar craton, and crustal averages.

The measured  $^{87}\text{Sr}/^{86}\text{Sr}$  ratios for the samples are highly variable (Table 2). The xenoliths have ratios from 0.70935 in the carbonate rock to as high as 0.78479 in the augen gneiss. The Rajmane dyke sample DND3, sampled away from xenoliths, shows a low ratio of 0.70465. Table 1 shows the ranges of initial  $^{87}\text{Sr}/^{86}\text{Sr}$  (at 66 Ma) for the lavas of the various Deccan stratigraphic formations in the Western Ghats. Using the low Rb/Sr of 0.072 for dyke DND3, which falls within the range of 0.01–0.34 for the Western Ghats lavas ( $n=624$ , Beane, 1988), we calculate  $^{87}\text{Rb}/^{86}\text{Sr}=0.2075$ , and the initial  $^{87}\text{Sr}/^{86}\text{Sr}$  at 66 Ma of 0.70445. This is only slightly lower than the present-day value. The initial  $^{87}\text{Sr}/^{86}\text{Sr}$  ratio is well within the Mahabaleshwar Formation range and just grabs the upper limit for the Ambenali Formation (Table 1), the formation least contaminated by continental lithospheric materials (e.g., Mahoney, 1988). The initial ratio is a little below the lower Sr isotopic limit for the Panhala Formation, and also conclusively precludes the dyke from representing any of the lower or middle formations in the Western Ghats stratigraphy, as also the Poladpur and Desur formations in the upper part of the stratigraphy, all of

which have much higher initial ratios reflecting significant lithospheric input.

For the xenoliths, similarly,  $^{87}\text{Sr}/^{86}\text{Sr}$  ratios calculated at 66 Ma are not very different from their measured values (Table 2), owing to low Rb/Sr ratios comparable to those of late Archaean granitoids (mostly monzogranites) of the Western Dharwar craton (Rb/Sr=0.19–5.99, though mostly  $\ll 1$ ) (Jayananda et al., 2006).

## 5. Discussion

What do the xenoliths in the Rajmane and Talwade dykes tell us about the basement immediately below? Because the two dykes are no longer than 5.5 km and 18 km, respectively, we believe that, even permitting lateral magma flow (see Ray et al., 2007), the xenoliths cannot have come from any great lateral distance. We therefore consider the xenoliths to be samples of the basement rocks directly under the dykes.

Based on deep seismic sounding work Kaila (1988) inferred the presence of a 1.8-km-thick Mesozoic sedimentary basin below the Deccan Traps in the region of the Tapi and Narmada rivers (Fig. 1). In the Pachmarhi area to the east (Fig. 1), tectonic uplift and erosional removal of the lava cover have spectacularly exposed this Mesozoic (Gondwana) basin, with its Deccan Trap intrusions (Sheth, 2007). The absence of any sedimentary material in the Rajmane and Talwade dykes probably suggests that the southern edge of the putative sub-Deccan Mesozoic sedimentary basin lies north of the dykes. Whereas the dykes are completely undeformed, the xenoliths (gneisses, mylonites, quartzites, granulite, tuff and metamorphosed carbonate) are dominantly metamorphic rocks. Mylonites typically indicate ductile shear zones, and granite mylonite, found here, is the most common type of mylonite (e.g., Best, 2003). The augen gneiss suggests a similar tectonic situation. These rocks are therefore products of regional metamorphism and shearing in a ductile shear zone.

Several major Proterozoic orogenic events affected the Archaean Indian shield but the shield has not been affected by orogenies after Proterozoic time (e.g., Leelanandam et al., 2006 and references therein). Therefore, we consider that the present xenolith suite comes from the Precambrian basement and not anything younger. The Pan-African orogeny at 600–500 Ma affected only the southern granulite terrain (e.g., Miller et al., 1996; Shabeer et al., 2005; Santosh et al., 2006; Ishii et al., 2006). The Proterozoic orogenic events described by Leelanandam et al. (2006) are close to the Eastern Indian coast. These areas are far from the central Deccan region and it is difficult to imagine their lithological and structural continuity under it.

Several studies have suggested the continuation of structures and rock types of the Dharwar craton into Deccan province (Drury and Holt, 1980; Gupta and Dwivedy, 1996; Dessai et al., 2004). At Latur (Fig. 1), the epicentre of a disastrous earthquake in 1993, drilling penetrated through a 338 m sequence of basalt and 8 m of sediment to reach a gneissic basement, equated to the Archaean Peninsular Gneiss of the Dharwar craton (Gupta and Dwivedy, 1996). The xenoliths described in this study are comparable to rocks of the Dharwar craton (see e.g., Dhoundial

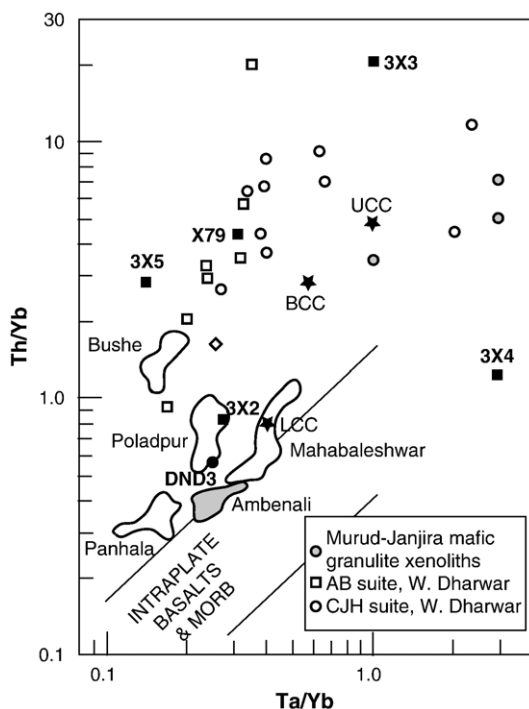


Fig. 7. Plot of Th/Yb vs. Ta/Yb for the dyke DND3 and the crustal xenoliths analyzed (this study), mafic granulite xenoliths from Murud–Janjira (Dessai et al., 2004), some Western Ghats formations (Lightfoot and Hawkesworth, 1988), late Archaean granitoids of the Western Dharwar craton (Jayananda et al., 2006), and crustal averages (UCC: upper continental crust, LCC: lower continental crust, BCC: bulk continental crust, Rudnick and Fountain, 1995).

et al., 1987; Chadwick et al., 2000, 2007). Chakrabarti and Basu (2006) have analyzed major and trace element and Sr–Nd–Pb isotopic compositions in impact breccia from the Lonar impact crater in the central Deccan (Fig. 1), 200 km southeast of Dhule, where again the basement is not exposed. They argue for an Archean basement and an extension of the Chitradurga schist belt, one of many such belts in the Dharwar craton (Fig. 1), under Lonar. There are several NNW-trending strike-slip crustal shear zones with large displacements documented in the Dharwar craton (e.g., Drury and Holt, 1980; Chadwick et al., 2000, 2007), though the proposed extension of the Chitradurga schist belt under Lonar (Chakrabarti and Basu, 2006) would require strike-slip displacement of several hundred kilometres along such shear zones, or alternatively a major swing in the trend of the fold belt. Nevertheless, the lithology and geochemistry available for the xenoliths of this study are consistent with the Archaean Dharwar craton, exposed south of the Deccan Traps, extending northward under the lavas for at least 350–400 km (see also Dessai et al., 2004).

Interestingly, and perhaps not surprisingly, all reported xenolith occurrences in the Deccan (Fig. 1) are in dykes, not lava flows. These comprise the granitic–quartzitic rafts at Mandaleshwar (Duraiswami and Karmalkar, 1996; Subbarao et al., 1999), granitic and broadly rhyolitic xenoliths near Ahmednagar (Sharma et al., 1999), lower crustal mafic and felsic granulites and (mantle) websterite and pyroxenite xenoliths at Murud–Janjira (Dessai et al., 2004), quartz–alkali feldspar–dolomite-bearing and partially assimilated xenoliths southwest of Mahabaleshwar (Mahoney, 1988), and quartz–alkali feldspar-bearing xenoliths at Sasaune (Dessai and Viegas, 1995). Perhaps the absence of xenoliths (as yet known) in Deccan lava flows has more to do with their getting filtered out during magma ascent in feeder dykes (depending on magma viscosities, flow rates, and xenolith–magma density contrasts) than a genuine absence to begin with.

## 6. Conclusions

The Rajmane and Talwade dykes in the central Deccan Traps, India, constitute rare and spectacular natural laboratories to study a great variety of xenoliths of Precambrian Indian crust. They thus provide invaluable windows into the basement of the Deccan Traps which lies mostly hidden over a huge (500,000 km<sup>2</sup>) expanse of these flood basalts. Our knowledge of this basement crust has necessarily been inferential, derived from geophysical (such as seismic and gravity) data and lava-dyke geochemistry. The new, direct evidence presented here from highly varied crustal xenoliths shows that the Precambrian crust below the central Deccan Traps is highly metamorphosed, tectonically deformed and lithologically heterogeneous on a small scale. Xenolith lithology and available geochemistry are consistent with the Archaean Dharwar craton, exposed south of the Deccan Traps, extending northward under the lavas for at least 350–400 km. This is significant for the evolution and constitution of the Precambrian Indian shield, as well as Precambrian palaeocontinental reconstructions (e.g., Rogers and Santosh, 2004).

## Acknowledgements

We thank the Industrial Research and Consultancy Centre, IIT Bombay for supporting the field work (grant 03IR014 to Sheth), and the Director, PRL, for allowing use of the PLANEX facility of the Indian Space Research Organization (ISRO) for major/trace element analysis. We also thank D. Gosain for field assistance, and D. Chandrasekharam, K. Pande, G. Mathew, and S. C. Patel for helpful discussions. This manuscript greatly benefitted from constructive, critical journal reviews by S. Arai and an anonymous reviewer, and the editorial input of T. Kusky and M. Santosh.

## References

- Barker, D.S., 2000. Emplacement of a xenolith-rich sill, Lajitas, Texas. *Journal of Volcanology and Geothermal Research* 104, 153–168.
- Beane, J.E., 1988. Flow stratigraphy, chemical variation and petrogenesis of Deccan flood basalts from the Western Ghats, India. Ph.D. dissertation. Washington State University, Pullman.
- Best, M.G., 2003. *Igneous and Metamorphic Petrology*, 2nd Edn. Blackwell Publ. 729 p.
- Bhaskar Rao, Y.J., Sivaraman, T.V., Pantulu, G.V.C., Gopalan, K., Naqvi, S.M., 1992. Rb–Sr ages of late Archaean metavolcanics and granites, Dharwar craton, South India and evidence for early Proterozoic thermotectonic event (s). *Precambrian Research* 59, 145–170.
- Bondre, N.R., Hart, W.K., Sheth, H.C., 2006. Geology and geochemistry of the Sangamner mafic dyke swarm, western Deccan volcanic province, India: implications for regional stratigraphy. *Journal of Geology* 114, 155–170.
- Chadwick, B., Vasudev, V.N., Hegde, G.V., 2000. The Dharwar craton, southern India, interpreted as the result of Late Archaean oblique convergence. *Precambrian Research* 99, 91–111.
- Chadwick, B., Vasudev, V.N., Hegde, G.V., Nutman, A.P., 2007. Structure and SHRIMP U/Pb zircon ages of granites adjacent to the Chitradurga schist belt: implications for Neoproterozoic convergence in the Dharwar craton, southern India. *Journal of Geological Society of India* 69, 5–24.
- Chakrabarti, R., Basu, A.R., 2006. Trace element and isotopic evidence for Archaean basement in the Lonar crater impact breccia, Deccan volcanic province. *Earth and Planetary Science Letters* 247, 197–211.
- Chandrasekharam, D., Mahoney, J.J., Sheth, H.C., Duncan, R.A., 1999. Elemental and Nd–Sr–Pb isotope geochemistry of flows and dikes from the Tapi rift, Deccan flood basalt province, India. *Journal of Volcanology and Geothermal Research* 93, 111–123.
- Chandrasekharam, D., Vaselli, O., Sheth, H.C., Keshav, S., 2000. Petrogenetic significance of ferro-enstatite orthopyroxene in basaltic dykes from the Tapi rift, Deccan flood basalt province. *Earth and Planetary Science Letters* 179, 469–476.
- Dessai, A.G., Viegas, A.A.A., 1995. Multi-generation mafic dyke swarm related to Deccan magmatism, south of Bombay: implications on the evolution of the western Indian continental margin. In: Devaraju, T.C. (Ed.), *Dyke Swarms of Peninsular India*. Geological Society of India Memoir 33, pp. 435–451.
- Dessai, A.G., Markwick, A., Vaselli, O., Downes, H., 2004. Granulite and pyroxenite xenoliths from the Deccan Trap: insight into the nature and composition of the lower lithosphere beneath cratonic India. *Lithos* 78, 263–290.
- Dhondial, D.P., Paul, D.K., Sarkar, A., Trivedi, J.R., Gopalan, K., Potts, P.J., 1987. Geochronology and geochemistry of Precambrian granitic rocks of Goa, SW India. *Precambrian Research* 36, 287–302.
- Drury, S.A., Holt, R.W., 1980. The tectonic framework of the South Indian craton: a reconnaissance involving LANDSAT imagery. *Tectonophysics* 65, T1–T15.
- Duraiswami, R.A., Karmalkar, N.R., 1996. Unusual xenolithic dyke at Mandaleshwar and its episodic nature. *Gondwana Geological Magazine* 11, 1–10.

- Farahat, E.S., Shaaban, M.M., Abdel Aal, A.Y., 2007. Mafic xenoliths from Egyptian Tertiary basalts and their petrogenetic implications. *Gondwana Research* 11, 516–528.
- Gao, S., Liu, X., Yuan, H., Hattendorf, B., Günther, D., Chen, L., Hu, S., 2002. Determination of forty two major and trace elements in USGS and NIST SRM glasses by laser ablation—inductively coupled plasma-mass spectrometry. *Geostandards Newsletter* 26, 181–196.
- Gupta, H.K., Dwivedy, K.K., 1996. Drilling at Latur earthquake region exposes a Peninsular Gneiss basement. *Journal of Geological Society of India* 47, 129–131.
- Ishii, S., Tsunogae, T., Santosh, M., 2006. Ultrahigh-temperature metamorphism in the Achankovil Zone: implications for the correlation of crustal blocks in southern India. In: Chetty, T.R.K., Fitzsimons, I., Brown, L., Dimri, V.P., Santosh, M. (Eds.), *Crustal Structure and Tectonic Evolution of the Southern Granulite Terrain, India*. *Gondwana Research* 10, pp. 99–114.
- Jayananda, M., Moya, J.-F., Martin, H., Peucat, J.-J., Auvray, J., Mahabaleswar, B., 2000. Late Archaean (2550–2520 Ma) juvenile magmatism in the Eastern Dharwar craton, southern India: constraints from geochronology, Nd–Sr isotopes and whole-rock geochemistry. *Precambrian Research* 99, 225–254.
- Jayananda, M., Chardon, D., Peucat, J.-J., Capdevila, R., 2006. 2.61 Ga potassic granites and crustal reworking in the western Dharwar craton, south India: tectonic, geochronologic and geochemical constraints. *Precambrian Research* 150, 1–26.
- Kaila, K.L., 1988. Mapping the thickness of Deccan Trap flows in India from DSS studies and inferences about a hidden Mesozoic sedimentary basin in the Narmada–Tapti region. In: Subbarao, K.V. (Ed.), *Deccan Flood Basalts*. *Geological Society of India Memoir* 10, pp. 91–116.
- Le Bas, M.J., Le Maitre, R.W., Streckeisen, A., Zanettin, B., 1986. A chemical classification of volcanic rocks on the total alkali–silica diagram. *Journal of Petrology* 27, 745–750.
- Leelanandam, C., Burke, K., Ashwal, L.D., Webb, S.J., 2006. Proterozoic mountain building in peninsular India: an analysis based primarily on alkaline rock distribution. *Geological Magazine* 143, 195–212.
- Lightfoot, P., Hawkesworth, C., 1988. Origin of Deccan Trap lavas: evidence from combined trace element and Sr-, Nd- and Pb-isotope studies. *Earth and Planetary Science Letters* 91, 89–104.
- Lightfoot, P.C., Hawkesworth, C.J., Devey, C.W., Rogers, N.W., van Calsteren, P.W.C., 1990. Source and differentiation of Deccan Trap lavas: implications of geochemical and mineral chemical variations. *Journal of Petrology* 31, 1165–1200.
- Mahadevan, T.M., 1994. Deep continental structure of India: a review. *Geological Society of India Memoir* 28 562 p.
- Mahoney, 1988. Deccan traps. In: Macdougall, J.D. (Ed.), *Continental Flood Basalts*. Kluwer Academic Publishers, Dordrecht, pp. 151–194.
- Mahoney, J.J., Macdougall, J.D., Lugmair, G.W., Murali, A.V., Sankar Das, M., Gopalan, K., 1982. Origin of Deccan trap flows at Mahabaleshwar inferred from Nd and Sr isotopic and chemical evidence. *Earth and Planetary Science Letters* 60, 47–60.
- Mahoney, J.J., Sheth, H.C., Chandrasekharam, D., Peng, Z.X., 2000. Geochemistry of flood basalts of the Toranmal section, northern Deccan Traps, India: implications for regional Deccan stratigraphy. *Journal of Petrology* 41, 1099–1120.
- Manikyamba, C., Khanna, T.C., 2007. Crustal growth processes as illustrated by the Neoproterozoic intraoceanic magmatism from Gadwal greenstone belt, Eastern Dharwar Craton, India. *Gondwana Research* 11, 476–491.
- Melluso, L., Barbieri, M., Beccaluva, L., 2004. Chemical evolution, petrogenesis, and regional chemical correlations of the flood basalt sequence in the central Deccan Traps, India. In: Sheth, H.C., Pande, K. (Eds.), *Magmatism in India through Time*. *Proceedings of the Indian Academy of Sciences (Earth & Planetary Sciences)* 113, pp. 587–603.
- Miller, J.S., Santosh, M., Pressley, R.A., Clements, A.S., Rogers, J.J.W., 1996. A Pan-African thermal event in southern India. *Journal of Asian Earth Sciences* 14, 127–136.
- Naqvi, S.M., Rogers, J.J.W., 1987. *Precambrian Geology of India*. Clarendon Press, New York.
- Pande, K., 2002. Age and duration of the Deccan Traps, India: a review of radiometric and palaeomagnetic constraints. *Proceedings of the Indian Academy of Sciences (Earth and Planetary Sciences)* 111, 115–123.
- Peng, Z.X., Mahoney, J., Hooper, P., Harris, C., Beane, J., 1994. A role for lower continental crust in flood basalt genesis? Isotopic and incompatible element study of the lower six formations of the western Deccan Traps. *Geochimica et Cosmochimica Acta* 58, 267–288.
- Radhakrishna, B.P., Naqvi, S.M., 1986. Precambrian continental crust of India and its evolution. *Journal of Geology* 94, 145–166.
- Rao, V.V., Reddy, P.R., 2002. A Mesoproterozoic supercontinent: evidence from the Indian shield. *Gondwana Research* 5, 63–74.
- Rai, S.N., Thiagarajan, S., 2007. 2-D crustal thermal structure along Thuadara–Sindad DSS profile across Narmada–Son lineament, central India. *Journal of Earth System Science* 116, 347–356.
- Ray, R., Sheth, H.C., Mallik, J., 2007. Structure and emplacement of the Nandurbar–Dhule mafic dyke swarm, Deccan Traps, and the tectonomagmatic evolution of flood basalts. *Bulletin of Volcanology* 69, 537–551.
- Rogers, J.J.W., Santosh, M., 2004. *Continents and Supercontinents*. Oxford University Press, New York. 289 p.
- Rudnick, R.L., 1992. Xenoliths—samples of the lower continental crust. In: Fountain, D.M., Arculus, R., Kay, R.W. (Eds.), *Continental Lower Crust*. *Developments in Tectonics* 23. Elsevier, pp. 269–316.
- Rudnick, R.L., Fountain, D.M., 1995. Nature and composition of the continental crust: a lower crustal perspective. *Reviews in Geophysics* 33, 267–309.
- Santosh, M., Tanaka, K., Yokoyama, K., Collins, A.S., 2005. Late Neoproterozoic–Cambrian felsic magmatism along transcrustal shear zones in southern India: U–Pb electron microprobe ages and implications for the amalgamation of the Gondwana Supercontinent. *Gondwana Research* 8, 31–42.
- Santosh, M., Collins, A.S., Tamashiro, I., Koshimoto, S., Tsutsumi, Y., Yokoyama, K., 2006. The timing of ultrahigh-temperature metamorphism in Southern India: U–Th–Pb electron microprobe ages from zircon and monazite in sapphirine-bearing granulites. In: Chetty, T.R.K., Fitzsimons, I., Brown, L., Dimri, V.P., Santosh, M. (Eds.), *Crustal Structure and Tectonic Evolution of the Southern Granulite Terrain, India*. *Gondwana Research* 10, pp. 128–155.
- Senthil Kumar, P., Menon, R., Reddy, G.K., 2007. The role of radiogenic heat production in the thermal evolution of a Proterozoic granulite-facies orogenic belt: Eastern Ghats, Indian shield. *Earth and Planetary Science Letters* 254, 39–54.
- Shabeer, K.P., Satish Kumar, M., Armstrong, R., Buick, I.S., 2005. Constraints on the timing of Pan-African granulite facies metamorphism in the Kerala khondalite belt of southern India: SHRIMP mineral ages and Nd isotopic systematics. *Journal of Geology* 113, 95–106.
- Sharma, R.K., Pandit, M.K., Warrior, S., 1999. Hybrid acid xenoliths in dolerite dykes intruding Deccan flood basalts, Pune–Ahmednagar region, western India. *Journal of Geological Society of India* 54, 303–308.
- Sheth, H.C., 2005. Were the Deccan flood basalts derived in part from ancient oceanic crust within the Indian continental lithosphere? *Gondwana Research* 8, 109–127.
- Sheth, H.C., 2007. Plume-related regional prevolcanic uplift in the Deccan Traps: absence of evidence, evidence of absence. In: Foulger, G.R., Jurdy, D.M. (Eds.), *Plates, Plumes, and Planetary Processes*. *Geological Society of America Special Paper* 430, pp. 785–814.
- Sheth, H.C., Pande, K. (Eds.), 2004. *Magmatism in India through Time*. *Proceedings of the Indian Academy of Sciences (Earth and Planetary Sciences)* 113, pp. 517–838 ([www.ias.ac.in/eps/contdec2004.html](http://www.ias.ac.in/eps/contdec2004.html)).
- Sheth, H.C., Mahoney, J.J., Chandrasekharam, D., 2004. Geochemical stratigraphy of Deccan flood basalts of the Bijasan Ghat section, Satpura Range, India. *Journal of Asian Earth Sciences* 23, 127–139.
- Subbarao, K.V., Hooper, P.R. (Compilers), 1988. Reconnaissance map of the Deccan Basalt Group in the Western Ghats, India. In: Subbarao, K.V. (Ed.), *Deccan Flood Basalts*. *Geological Society of India Memoir* 10, (enclosure).
- Subbarao, K.V., Chandrasekharam, D., Navaneethakrishnan, P., Hooper, P.R., 1994. Stratigraphy and structure of parts of the central Deccan basalt province: eruptive models. In: Subbarao, K.V. (Ed.), *Volcanism*. Wiley Eastern Ltd., New Delhi, pp. 321–332 (Compilers).
- Subbarao, K.V., Hooper, P.R., Dayal, A.M., Walsh, J.N., Gopalan, K., 1999. Narmada dykes. In: Subbarao, K.V. (Ed.), *Deccan Volcanic Province*. *Geological Society of India Memoir* 43(2), pp. 891–902.
- Sun, S.-S., McDonough, W.F., 1989. Chemical and isotopic systematics of oceanic basalts: implications for mantle composition and processes. In:

- Saunders, A.D., Norry, M.J. (Eds.), *Magmatism in the Ocean Basins*. Geological Society of London Special Publication 42, pp. 313–345.
- Vanderkluisen, L., Mahoney, J.J., Hooper, P.R., Sheth, H.C., 2006. Location and geometry of the Deccan traps feeder system inferred from dyke geochemistry. *Eos, Transactions of the American Geophysical Union*. Fall Meeting Supplement 87 (52), p. V13B–0681. abstract.
- Weis, D., Kieffer, B., Maerschalk, C., Pretorius, W., Barling, J., 2005. High-precision Pb–Sr–Nd–Hf isotopic characterization of USGS BHVO-1 and BHVO-2 reference materials. *Geochemistry, Geophysics, Geosystems* 6. doi:10.1029/2004GC000852.